Respiratory Motion Imaging Using 2.4-GHz Nine-Element-Array Continuous-Wave Radar

Sakamoto, Takuya; Koda, Takato

Respiratory Motion Imaging Using 2.4-GHz Nine-Element-Array Continuous-Wave Radar

Takuya Sakamoto, *Senior Member, IEEE*, and Takato Koda

***Abstract*— A radar system with antenna array and signal processing method are presented for noncontact monitoring of human respiration. We develop a 2.4-GHz nine-element radar system and use it to measure the respiratory rate of a participant lying on a bed. The results show that this system and method can image a respiring body and estimate its instantaneous respiration rate accurately. The accuracy of the proposed system is validated by simultaneously recording the ribcage circumference using a piezoelectric respiratory sensor and the 3-D body shape using a depth camera. The results indicate the potential of this system for long-term respiratory monitoring during sleep periods.**

***Index Terms*— Antenna array, microwave, radar imaging, respiration.**

I. Introduction

MEASURING vital signs and physiological signals such as heartbeat and respiration is very important in healthcare applications. Noncontact measurements of vital signs using radar systems do not cause skin irritation or discomfort as contact measurements do. Radar-based measurements also cause less concern about privacy than camera-based measurements. For these reasons, radar-based sleep monitoring is a promising approach to long-term measurement of vital signs.

To estimate the direction of arrival of vital echoes, Wang *et al.* [1] and Peng *et al.* [2] studied mechanical antenna rotation with a 5.8-GHz radar system and Chen *et al.* [3] studied mechanical antenna scanning with a 1.5-GHz ultra-wideband (UWB) radar system. Because radar systems with mechanical rotation/scanning are generally bulky and heavy, array antennas are preferable in such applications.

Millimeter-wave radar systems have become more widely used to monitor physiological signals. Islam *et al.* [4] used a 24-GHz two-element radar system to monitor the respiration of two people. Walterscheid *et al.* [5] located a number of people through their breathing with a radar system operating at 24-GHz with 16 channels and another operating at 77-GHz with 32 channels in multiple-input–multiple-output (MIMO) mode. Our group [6] used a 60-GHz eight-channel MIMO radar system to measure a heartbeat.

Manuscript received April 11, 2020; accepted May 1, 2020. Date of publication May 21, 2020; date of current version July 7, 2020. This work was supported in part by the Japan Society for the Promotion of Science (JSPS) KAKENHI under Grant 19H02155, in part by Japan Science and Technology Agency (JST) Precursory Research for Embryonic Science and Technology (PRESTO) under Grant JPMJPR1873, and in part by the JST Center of Innovation (COI) under Grant JPMJCE1307. *(Corresponding author: Takuya Sakamoto.)*

The authors are with the Department of Electrical Engineering, Graduate School of Engineering, Kyoto University, Kyoto 615-8510, Japan (e-mail: sakamoto.takuya.8n@kyoto-u.ac.jp).

Color versions of one or more of the figures in this letter are available online at http://ieeexplore.ieee.org.

Digital Object Identifier 10.1109/LMWC.2020.2992541

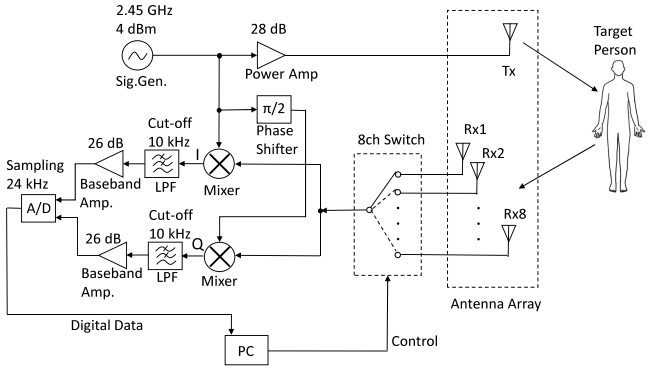

Fig. 1. Block diagram of the radar system.

On the other hand, lower frequency microwave radar systems with antenna array have the advantage of easily penetrating thick clothing and comforters to measure physiological signals even when a person is wrapped in a thick quilt. Hsu *et al.* [7] built a 2.4-GHz four-element radar using self-injection-locked radar. Mostafanezhad *et al.* [8] built a 2.4-GHz four-element radar system using a time-domain multiplexing circuit to measure respiration of a single person. Hall *et al.* [9] and Boothby *et al.* [10] built a 2.4-GHz three-element radar system that can find the direction with the largest phase fluctuation.

Despite these studies to develop radar systems with antenna array to monitor respiration, no reported system can identify a specific body part (e.g., chest wall or abdomen) through respiratory motion. Locating that part of the body moving at a respiratory rate would help in detecting and monitoring respiratory illnesses including sleep apnea. In this letter, we designed and fabricated the first 2.4-GHz continuous wave (CW) radar system coupled with a 2-D nine-element antenna array that accurately locates a respiring body of a sleeping person. The measurement results indicate the effectiveness of our radar system with antenna array in imaging and measuring respiration.

II. Radar With Cross-Shaped Array

Our radar system (see Fig. 1) has a single transmit element and eight receive elements for a total of nine elements. The eight receive elements are connected to an eight-port GaAs integrated-circuit switch. The antenna array is cross-shaped as shown in Fig. 2, where the transmit element is at the center and the receive elements form a cross around it. Each element is an omnidirectional ceramic patch antenna with a peak gain of 2 dBi. The element intervals are all 7.0 cm, which corresponds

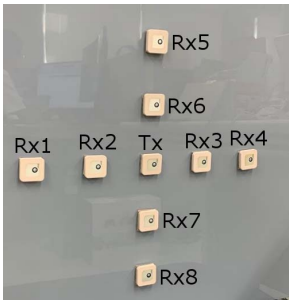

Fig. 2. Radar with antenna array designed and used in this letter.

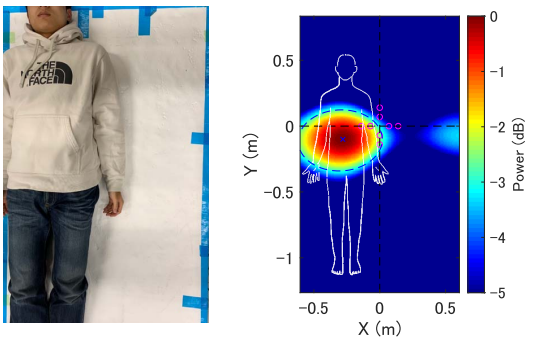

Fig. 3. Participant lying on the left side of the bed (left) and radar image focusing on the respiratory motion (right).

to 0.57λ, where $\lambda = 12.3$ cm is the wavelength for 2.45 GHz. The position of the ith receive element is denoted as $(x_i, y_i, 0)$ for $i = 1, \ldots, N$, where $N = 8$ and the transmit element is at the origin. The received signals go through the GaAs switch and are down-converted by a pair of mixers. The transmit signal is also fed to the mixers via a quadrature hybrid coupler. Then, their I and Q components are A/D converted using a data acquisition (DAQ) hardware. The sampling frequency of the A/D converter is 24 kHz. The A/D converted data are averaged and decimated by a factor of 30, resulting in 800 Hz sampling. Because there are $N = 8$ channels, the sampling frequency for each channel becomes 100 Hz. For example, assuming a sinusoidal respiration motion with an amplitude of 2 mm and a period of 5 s, the maximum Doppler shift is 0.04 Hz, which is much lower than the sampling frequency.

III. Radar Measurement With a Participant

The radar system was installed above a Styrofoam bed. The top surface of the bed was 1.25 m below the array that was facing down to the floor. First, we used the radar system to measure an empty scene without a participant to obtain the background echo signal vector $\boldsymbol{s}^{(\mathrm{bg})}(t) = [s_1^{(\mathrm{bg})}(t), \cdots, s_N^{(\mathrm{bg})}(t)]^{\mathrm{T}}$ containing a direct-current component caused by static clutter, where superscript T denotes the matrix transpose, and $N = 8$ is the number of receive elements. Because these background signals are time-invariant, they are averaged over time via $\bar{\boldsymbol{s}}^{(\mathrm{bg})} = (1/T)\int_0^T \boldsymbol{s}^{(\mathrm{bg})}(t)\mathrm{d}t$, where T is the total measurement time.

Next, we measured a participant lying on the bed and obtained the echo signal vector $\boldsymbol{s}'(t)$. The participant was a healthy male in his twenties. The participant was instructed to remain calm and stationary and to breathe normally during the measurement for $T = 60.0$ s. To estimate the respiration period, the measurement time T needs to be twice longer than the respiration period. Because a typical respiration period is 5 s, T must be longer than 10 s. The background echo signal $\bar{\boldsymbol{s}}^{(\mathrm{bg})}$ is subtracted via $\boldsymbol{s}(t) = \boldsymbol{s}'(t) - \bar{\boldsymbol{s}}^{(\mathrm{bg})}$, and $\boldsymbol{s}(t)$ is processed in Section IV.

IV. Radar Imaging of Respiratory Motion

To selectively obtain an image associated with respiratory motion only, our proposed method obtains image $I(x, y)$ via

$$I(x, y) = \int_0^T \left| \boldsymbol{w}(x, y)^{\mathrm{H}} \int_0^T h(t - \tau)\boldsymbol{s}(\tau)\mathrm{d}\tau \right|^2 \mathrm{d}t \qquad (1)$$

where superscript H denotes the Hermitian transpose, $h(t)$ is the inverse Fourier transform of a bandpass filter $H(\omega)$ to retrieve the respiration component. $H(\omega)$ is defined as $H(\omega) = 1$ for $\omega_{\mathrm{L}} \le \omega \le \omega_{\mathrm{H}}$, and $H(\omega) = 0$ otherwise. Here, ω_{L} and $\omega_{\mathrm{H}} (> \omega_{\mathrm{L}})$ are half-power angular frequencies of the signal spectrum $S(\omega)$ that is obtained by averaging spectra calculated from eight channels. The beam-forming weight vector $\boldsymbol{w}(x, y)$ is defined as $\boldsymbol{w}(x, y) = [w_1(x, y), w_2(x, y), \ldots, w_N(x, y)]^{\mathrm{T}}$, whose elements $w_i(x, y) = \mathrm{e}^{\mathrm{j}k((x_i - x)^2 + (y_i - y)^2 + z_0^2)^{1/2}}$ $(i = 1, \ldots, N)$ compensate for the phase rotation caused by propagation. The beam-forming weight $\boldsymbol{w}(x, y)$ focuses signals to position (x, y, z_0), where z_0 is the distance between the array plane and the bed.

The filter $H(\omega)$ is designed on the basis of the respiration characteristic of the target person estimated from the power spectrum of the echo signal. By introducing bandpass filter $H(\omega)$, we can obtain a radar image $I(x, y)$ of a specific body part showing respiratory motion such as the chest wall or abdomen.

Next, we determine the representative position of respiratory motion by finding the maxima of the image $I(x, y)$ via $(x_0, y_0) = \arg\max_{(x,y)} I(x, y)$. We then obtain the displacement of the body part at (x_0, y_0, z_0) that is expected to contain the largest respiration component via

$$r_0(t) = (\lambda/4\pi)\angle\left(\boldsymbol{w}(x_0, y_0)^{\mathrm{H}}\boldsymbol{s}(t)\right). \qquad (2)$$

Displacement $r_0(t)$ is expected to be more accurate than a displacement estimated using a single-channel signal without an antenna array.

V. Application of the Proposed Imaging Method

We next apply our imaging method to the measured radar signals. Figs. 3 and 4 show photographs of a participant lying face-up on a bed and radar images produced using the proposed method. The difference between Figs. 3 and 4 is the reverse orientation of the participant. These figures indicate the performance accuracy of the imaging system. The spatial 3-dB resolutions of these images are 0.57 and 0.69 m, respectively. The resolution was defined as the average of the major and minor axes of an ellipse that is fit to the −3-dB contour line extracted from the image and shown as dashed

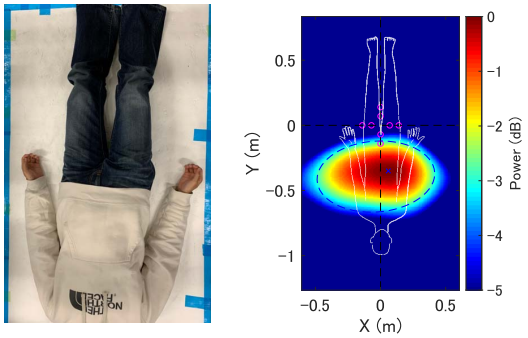

Fig. 4. Participant lying upside-down on the bed (left) and radar image focusing on the respiratory motion (right).

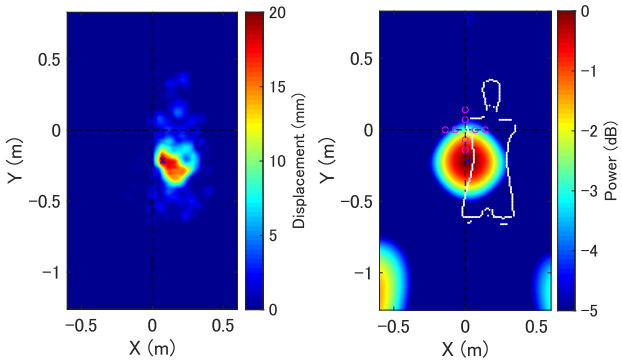

Fig. 5. Participant lying on the right side of the bed (left) and radar image focusing on the respiratory motion (right).

curves. Note that the image resolution depends on the distance from the radar to the participant.

To verify the imaging accuracy, we introduced an Intel RealSense depth camera (Intel Corporation, Santa Clara, CA, USA) to record the actual body displacement of the participant. In this measurement, the participant was in tight and thin underwear only so that the depth camera could detect the actual body shape and skin displacement accurately. The depth camera recording was done only to evaluate the performance of the radar-based system in this letter. In general practice, only the radar system will be used and users undergoing tests can be in clothes and on a bed. We assume that the depth camera images are sufficiently accurate to be used as a reference.

Fig. 5 shows the body displacement image (left) obtained using a depth camera and the radar image $I(x, y)$ (right). Note that the silhouette line of the human body is shown only for readers' convenience and it is not necessarily accurate. The blue cross symbols are the peak position with the largest respiratory motion. The discrepancy between the peaks in the radar and depth camera images was 0.05 m. These discrepancies without the bandpass filter was 0.07 m. These results indicate that the proposed imaging method in (1) improved the spatial accuracy by a factor of 1.4.

VI. Respiration Measurement Validation Using Contact Sensor

We investigated the accuracy in measuring the respiration rate using (2). To assess the accuracy, we also measured the

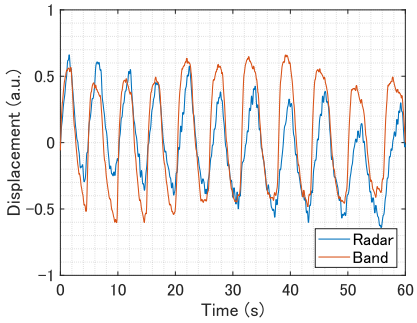

Fig. 6. Body displacement measured using the proposed bandpass-filtered beam-forming radar imaging (blue) and piezoelectric respiration sensor belt (red) with the participant on the right side of the bed.

change in the ribcage circumference of the participant using a piezoelectric respiratory effort sensor with a chest belt as a reference. Fig. 6 shows the chest belt data (blue) and radar data (red) obtained using (2) for the same measurement as Fig. 5. Although these curves do not match exactly, their temporal periodic patterns are almost identical. We obtained time-dependent instantaneous respiration intervals (RIs) by applying a local auto-correlation method to both data. The root-mean-square (rms) error of the RIs calculated from the radar and chest belt data was calculated to be 30 ms, which is sufficiently small compared with the respiration period. Next, to investigate the improvement in accuracy due to the proposed antenna array, we estimated the RI using only a single element instead of eight; the rms error was 135 ms on average using a single element, indicating a 4.5-fold improvement in accuracy. The results show the effectiveness of our proposed system for monitoring respiratory patterns.

VII. Conclusion

We designed and fabricated a 2.4-GHz nine-element radar system for use in measuring a participant lying on a bed below the array antenna. We also proposed a radar imaging method specifically targeting the respiratory component by introducing a bandpass filter before forming an image. This method was applied to the measured radar data and the images obtained depicting the chest wall and abdomen of the participant. We conducted a measurement using a depth camera and a piezoelectric respiratory sensor to assess the accuracies in imaging and estimating the respiration rate. The result gave an average imaging error of 0.05 m and error of 30 ms in estimating the RI, which indicates the effectiveness of the designed radar system and imaging method. This system, which has more antenna elements than existing 2.4-GHz radar systems [7]–[10], generated for the first time an image from respiratory motion. The performance of this system will be evaluated with more data sets involving more participants in future work. Although we used only a low-cost CW radar system in this letter, the next important step would involve the use of frequency-modulated CW radar [11], [12] to achieve a higher resolution in respiratory imaging.

References

[1] G. Wang, C. Gu, T. Inoue, and C. Li, "A hybrid FMCW-interferometry radar for indoor precise positioning and versatile life activity monitoring," *IEEE Trans. Microw. Theory Techn.*, vol. 62, no. 11, pp. 2812–2822, Nov. 2014.

[2] Z. Peng *et al.*, "A portable FMCW interferometry radar with programmable low-IF architecture for localization, ISAR imaging, and vital sign tracking," *IEEE Trans. Microw. Theory Techn.*, vol. 65, no. 4, pp. 1334–1344, Apr. 2017, doi: 10.1109/TMTT.2016.2633352.

[3] T.-C. Chen, J.-H. Liu, P.-Y. Chao, and P.-C. Li, "Ultrawideband synthetic aperture radar for respiratory motion detection," *IEEE Trans. Geosci. Remote Sens.*, vol. 53, no. 7, pp. 3749–3763, Jul. 2015, doi: 10.1109/TGRS.2014.2382672.

[4] S. M. M. Islam, E. Yavari, A. Rahman, V. M. Lubecke, and O. Boric-Lubecke, "Separation of respiratory signatures for multiple subjects using independent component analysis with the JADE algorithm," in *Proc. 40th Annu. Int. Conf. IEEE Eng. Med. Biol. Soc. (EMBC)*, Honolulu, HI, USA, Jul. 2018.

[5] I. Walterscheid, O. Biallawons, and P. Berens, "Contactless respiration and heartbeat monitoring of multiple people using a 2-D imaging radar," in *Proc. 41st Annu. Int. Conf. IEEE Eng. Med. Biol. Soc. (EMBC)*, Berlin, Germany, Jul. 2019, doi: 10.1109/EMBC.2019.8856974.

[6] T. Sakamoto and K. Yamashita, "Noncontact measurement of autonomic nervous system activities based on heart rate variability using ultra-wideband array radar," *IEEE J. Electromagn., RF Microw. Med. Biol.*, early access, Oct. 22, 2019, doi: 10.1109/JERM.2019.2948827.

[7] C.-Y. Hsu, C.-Y. Chuang, F.-K. Wang, T.-S. Horng, and L.-T. Hwang, "Detection of vital signs for multiple subjects by using self-injection-locked radar and mutually injection-locked beam scanning array," in *IEEE MTT-S Int. Microw. Symp. Dig.*, Honolulu, HI, USA, Jun. 2017, pp. 991–994.

[8] I. Mostafanezhad, E. Yavari, and O. Boric-Lubecke, "A low cost simple RF front end using time-domain multiplexing for direction of arrival estimation of physiological signals," in *IEEE MTT-S Int. Microw. Symp. Dig.*, Seattle, WA, USA, Jun. 2013, pp. 1–4.

[9] T. Hall *et al.*, "A phased array non-contact vital signs sensor with automatic beam steering," in *IEEE MTT-S Int. Microw. Symp. Dig.*, Phoenix, AZ, USA, May 2015, pp. 1–4.

[10] A. Boothby *et al.*, "Accurate and continuous non-contact vital signs monitoring using phased array antennas in a clutter-free anechoic chamber," in *Proc. 35th Annu. Int. Conf. IEEE Eng. Med. Biol. Soc. (EMBC)*, Osaka, Japan, Jul. 2013, pp. 2862–2865.

[11] F. Adib, H. Mao, Z. Kabelac, D. Katabi, and R. C. Miller, "Smart homes that monitor breathing and heart rate," in *Proc. 33rd Annu. ACM Conf. Hum. Factors Comput. Syst. (CHI)*, Seoul, South Korea, Apr. 2015, pp. 837–846, doi: 10.1145/2702123.2702200.

[12] M. Hiraki *et al.*, "Millimeter-wave cost-effective phased-array radar with orthogonally located linear Tx and Rx arrays," in *IEEE MTT-S Int. Microw. Symp. Dig.*, Boston, MA, USA, Jun. 2019, pp. 540–543, doi: 10.1109/MWSYM.2019.8701078.